

This is an Open Access document downloaded from ORCA, Cardiff University's institutional repository:<https://orca.cardiff.ac.uk/id/eprint/128372/>

This is the author's version of a work that was submitted to / accepted for publication.

Citation for final published version:

Cattaneo, Stefano, Bonincontro, Danilo, Bere, Takudzwa, Kiely, Christopher J. , Hutchings, Graham J. , Dimitratos, Nikolaos and Albonetti, Stefania 2020. Continuous flow synthesis of bimetallic AuPd catalysts for the selective oxidation of 5-hydroxymethylfurfural to 2,5-furandicarboxylic acid. *ChemNanoMat* 6 (3) , pp. 420-426. 10.1002/cnma.201900704

Publishers page: <http://dx.doi.org/10.1002/cnma.201900704>

Please note:

Changes made as a result of publishing processes such as copy-editing, formatting and page numbers may not be reflected in this version. For the definitive version of this publication, please refer to the published source. You are advised to consult the publisher's version if you wish to cite this paper.

This version is being made available in accordance with publisher policies. See <http://orca.cf.ac.uk/policies.html> for usage policies. Copyright and moral rights for publications made available in ORCA are retained by the copyright holders.



Supplementary on-line information

Continuous flow synthesis of bimetallic AuPd catalysts for the selective oxidation of 5-hydroxymethylfurfural to 2,4-furandicarboxylic acid

Stefano Cattaneo*,^{[a][b]} Danilo Bonincontro,^[c] Takudzwa Bere,^[a] Christopher J. Kiely,^{[a][d]} Graham J. Hutchings,^[a] Nikolaos Dimitratos^{[a][c]} and Stefania Albonetti*^[c]

[a] Dr. S. Cattaneo, T. Bere, Prof. C. J. Kiely, Prof. G. J. Hutchings and Prof. N. Dimitratos

Cardiff Catalysis Institute, School of Chemistry

Cardiff University

CF10 3AT, Cardiff, UK

E-mail: Stefano.Cattaneo2@unimi.it

BereT@cardiff.ac.uk

Chk5@lehigh.edu

Hutch@cardiff.ac.uk

Nikolaos.Dimitratos@unibo.it

[b] Dr. S. Cattaneo

Dipartimento di Chimica

Università degli Studi di Milano

Via Golgi 19

20133, Milano, Italy

[c] Dr. D. Bonincontro, Prof. S. Albonetti

"Toso Montanari" Department of Industrial Chemistry

University of Bologna

Viale Risorgimento 4

40136, Bologna, Italy

E-mail: Danilo.Bonincontro@unibo.it

Stefania.Albonetti@unibo.it

Nikolaos.Dimitratos@unibo.it

[d] Prof. C. J. Kiely

Department of Materials Science and Engineering

Lehigh University

5 East Packer Avenue

Bethlehem, Pennsylvania, PA 18015, USA

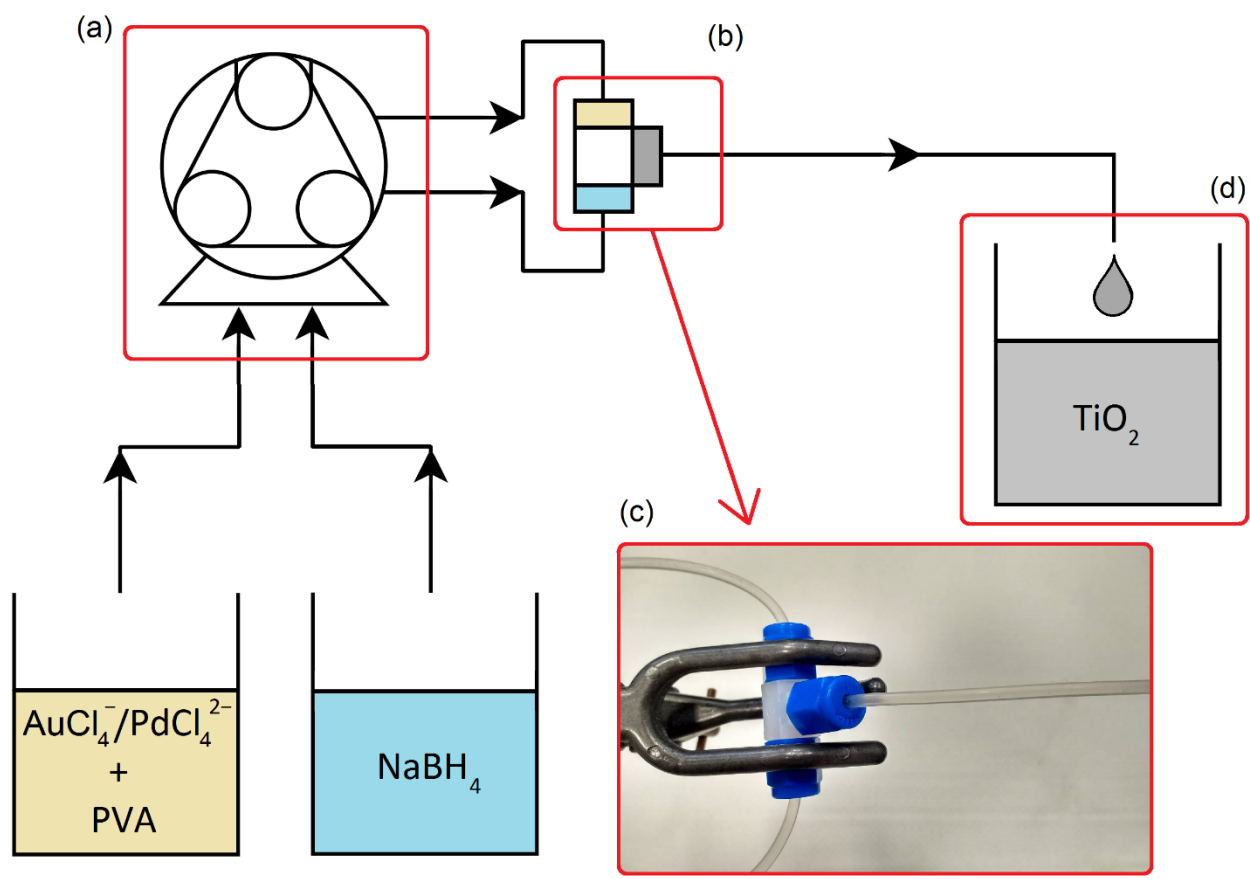


Figure S1: Schematic representation of the millifluidic set-up for the synthesis of $\text{Au}_x\text{Pd}_y/\text{TiO}_2$ catalysts in continuous mode. (a) Peristaltic pump, (b) PFA T-shape connection, (c) image of the PFA T-shape connection and (d) suspension of TiO_2 in water.

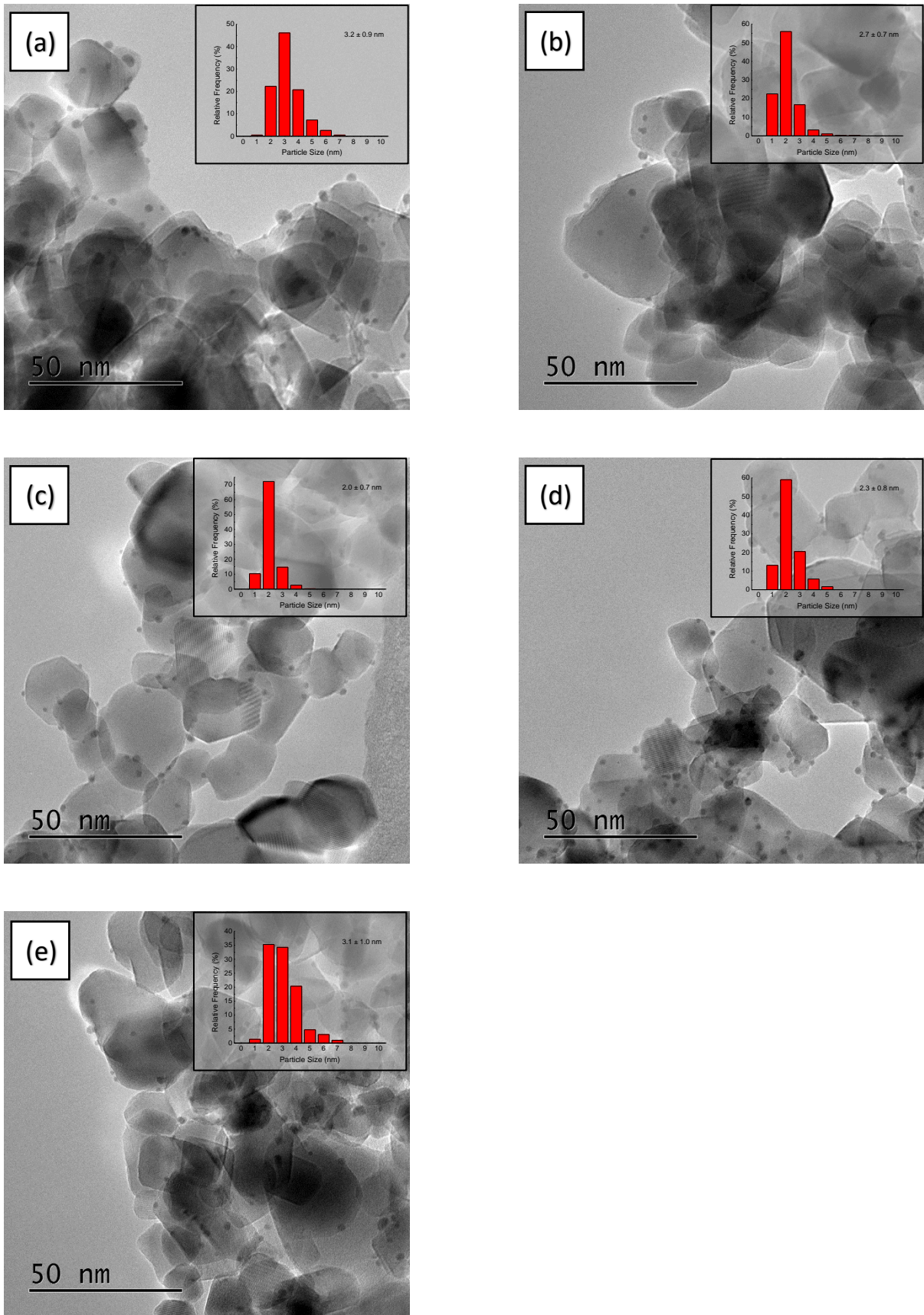


Figure S2: Representative BF-TEM images and (inset) respective particle size distributions of the various catalysts prepared in continuous mode: (a) Au/TiO₂, (b) Au₇₅Pd₂₅/TiO₂, (c) Au₅₀Pd₅₀/TiO₂, (d) Au₂₅Pd₇₅/TiO₂ and (e) Pd/TiO₂.

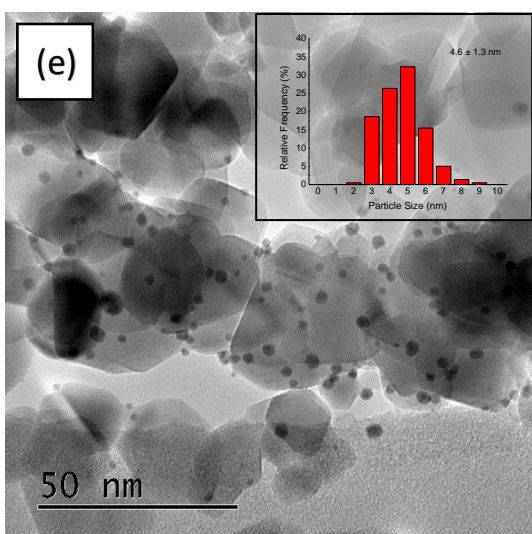
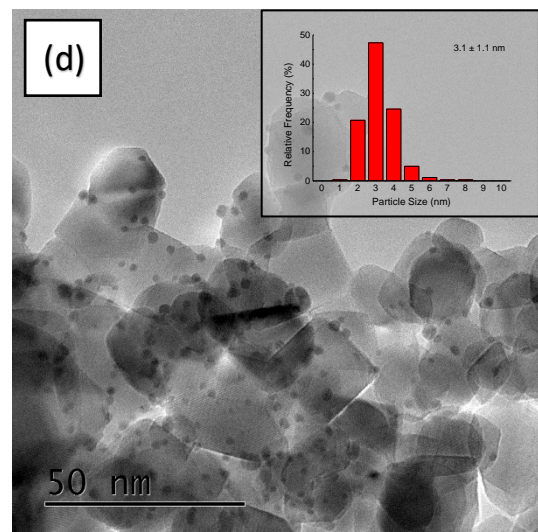
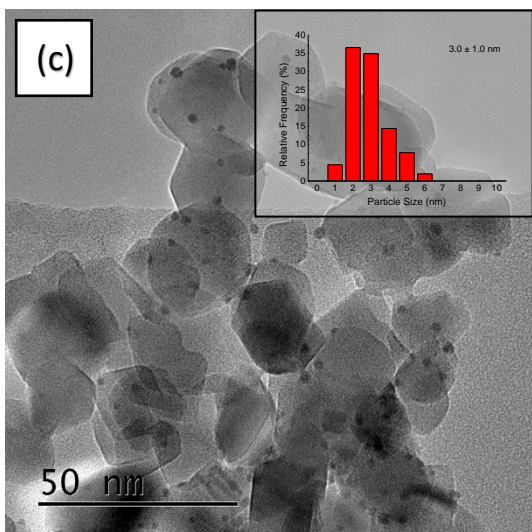
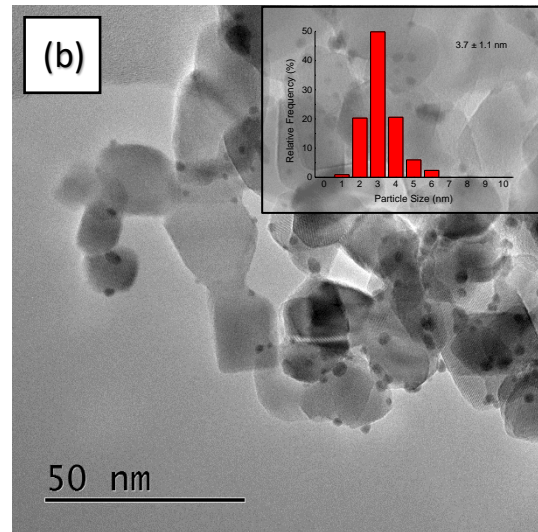
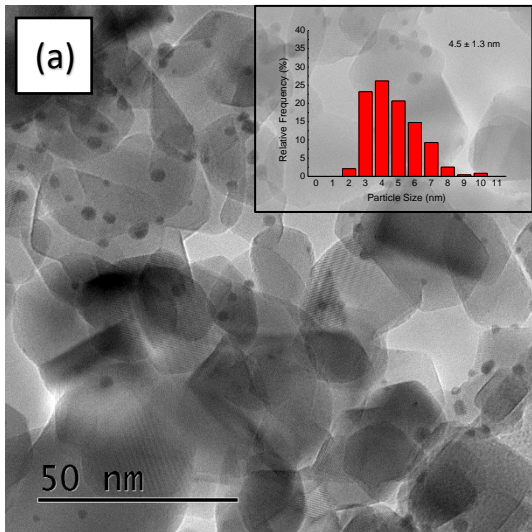


Figure S3: Representative BF-TEM images and (inset) the respective particle size distribution of the various catalysts prepared in batch mode: (a) Au/TiO_2 , (b) $\text{Au}_{75}\text{Pd}_{25}/\text{TiO}_2$, (c) $\text{Au}_{50}\text{Pd}_{50}/\text{TiO}_2$, (d) $\text{Au}_{25}\text{Pd}_{75}/\text{TiO}_2$ and (e) Pd/TiO_2 .

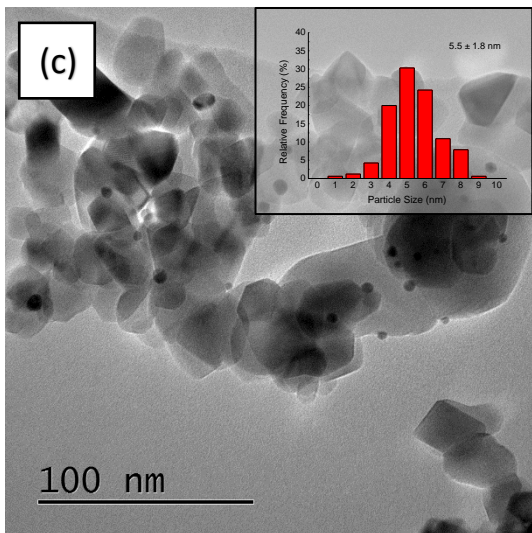
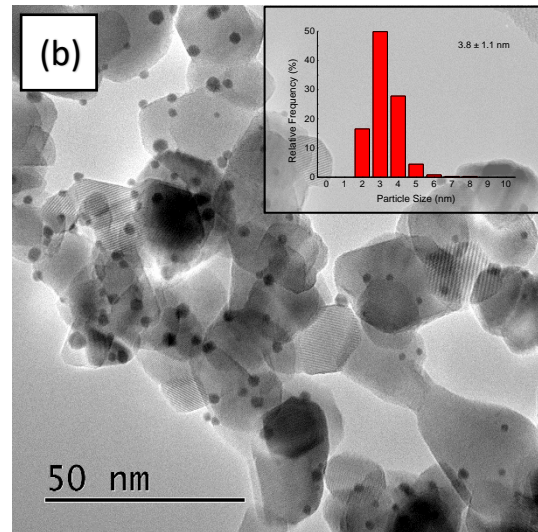
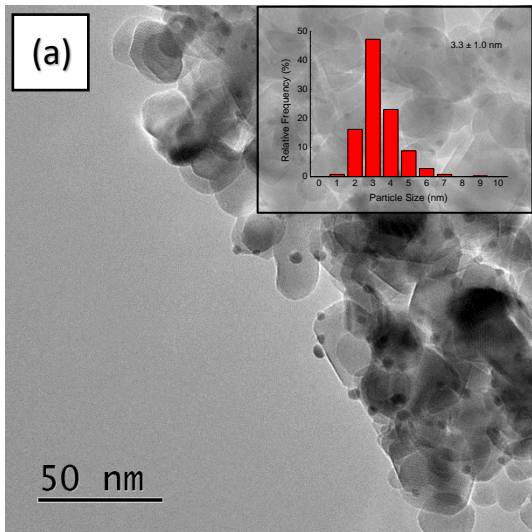


Figure S4: Representative BF-TEM images and (inset) the respective particle size distributions of the $\text{Au}_{75}\text{Pd}_{25}/\text{TiO}_2$ catalyst prepared in continuous mode and subjected to thermal calcination treatment at (a) 200°C , (b) 300°C and (c) 400°C .

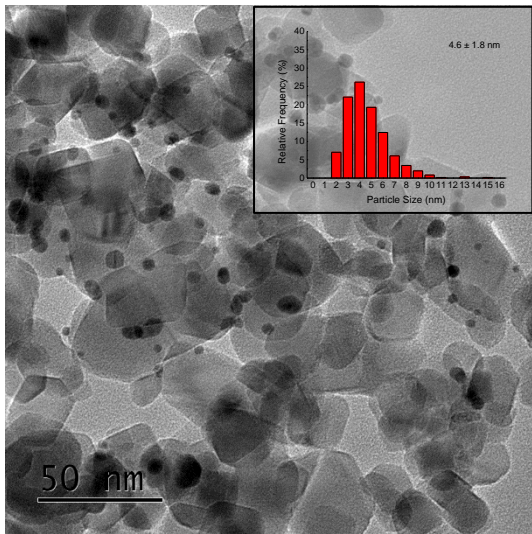


Figure S5: Representative BF-TEM image of the $\text{Au}_{75}\text{Pd}_{25}/\text{TiO}_2$ catalyst prepared in continuous mode and heat treated at 200°C after the 5th catalysis run. The particle size distribution is shown in the inset.

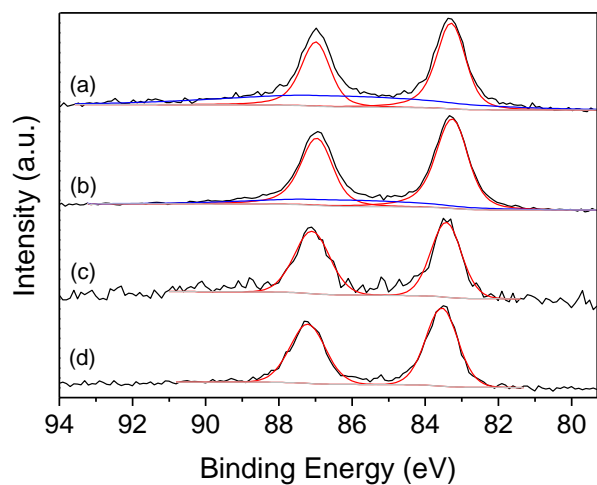


Figure S6: Au4f XPS analysis of the batch-prepared catalysts. (a) $\text{Au}_{25}\text{Pd}_{75}/\text{TiO}_2$, (b) $\text{Au}_{50}\text{Pd}_{50}/\text{TiO}_2$, (c) $\text{Au}_{75}\text{Pd}_{25}/\text{TiO}_2$ and (d) Au/TiO_2 . The red fitting represents the Au^0 , while the blue fitting represents the satellite Pd 4s peak.

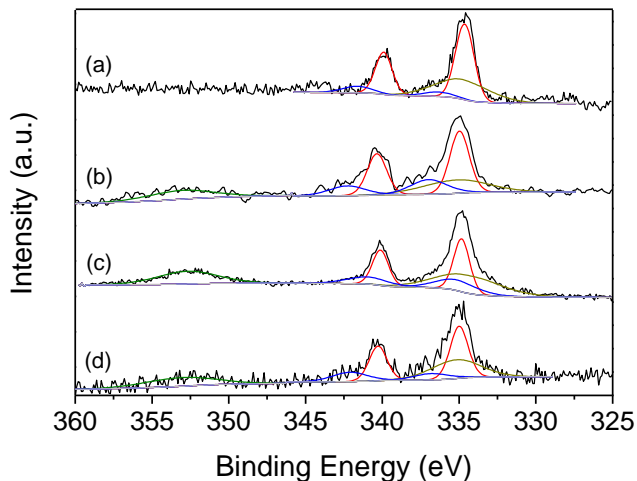


Figure S7: Pd3d XPS analysis of the batch-prepared catalysts. (a) Pd/TiO_2 , (b) $\text{Au}_{25}\text{Pd}_{75}/\text{TiO}_2$, (c) $\text{Au}_{50}\text{Pd}_{50}/\text{TiO}_2$ and (d) $\text{Au}_{75}\text{Pd}_{25}/\text{TiO}_2$. The red fitting represents the Pd^0 , while the blue fitting represents the Pd^{2+} ; the green fitting represents the satellite Au 4d peaks.

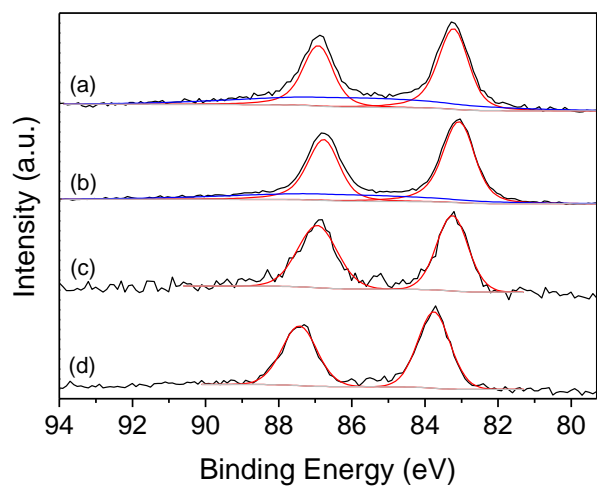


Figure S8: Au4f XPS analysis of the continuous-prepared catalysts. (a) $\text{Au}_{25}\text{Pd}_{75}/\text{TiO}_2$, (b) $\text{Au}_{50}\text{Pd}_{50}/\text{TiO}_2$, (c) $\text{Au}_{75}\text{Pd}_{25}/\text{TiO}_2$ and (d) Au/TiO_2 . The red fitting represents the Au^0 , while the blue fitting represents the satellite Pd 4s peak.

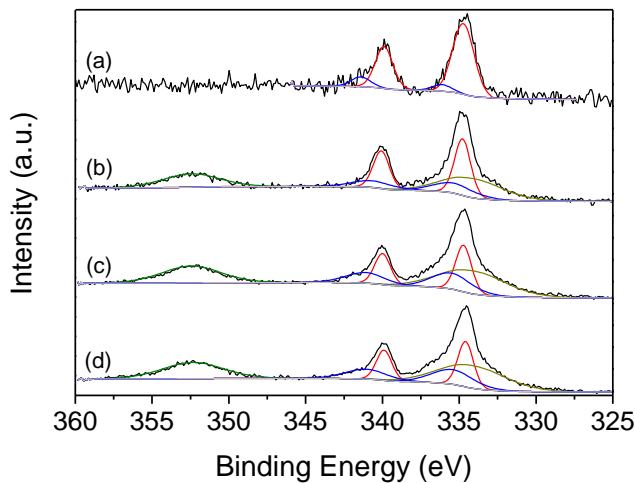


Figure S9: Pd3d XPS analysis of the continuous-prepared catalysts. (a) Pd/TiO_2 , (b) $\text{Au}_{25}\text{Pd}_{75}/\text{TiO}_2$, (c) $\text{Au}_{50}\text{Pd}_{50}/\text{TiO}_2$ and (d) $\text{Au}_{75}\text{Pd}_{25}/\text{TiO}_2$. The red fitting represents the Pd^0 , while the blue fitting represents the Pd^{2+} ; the green fitting represents the satellite Au 4d peaks.

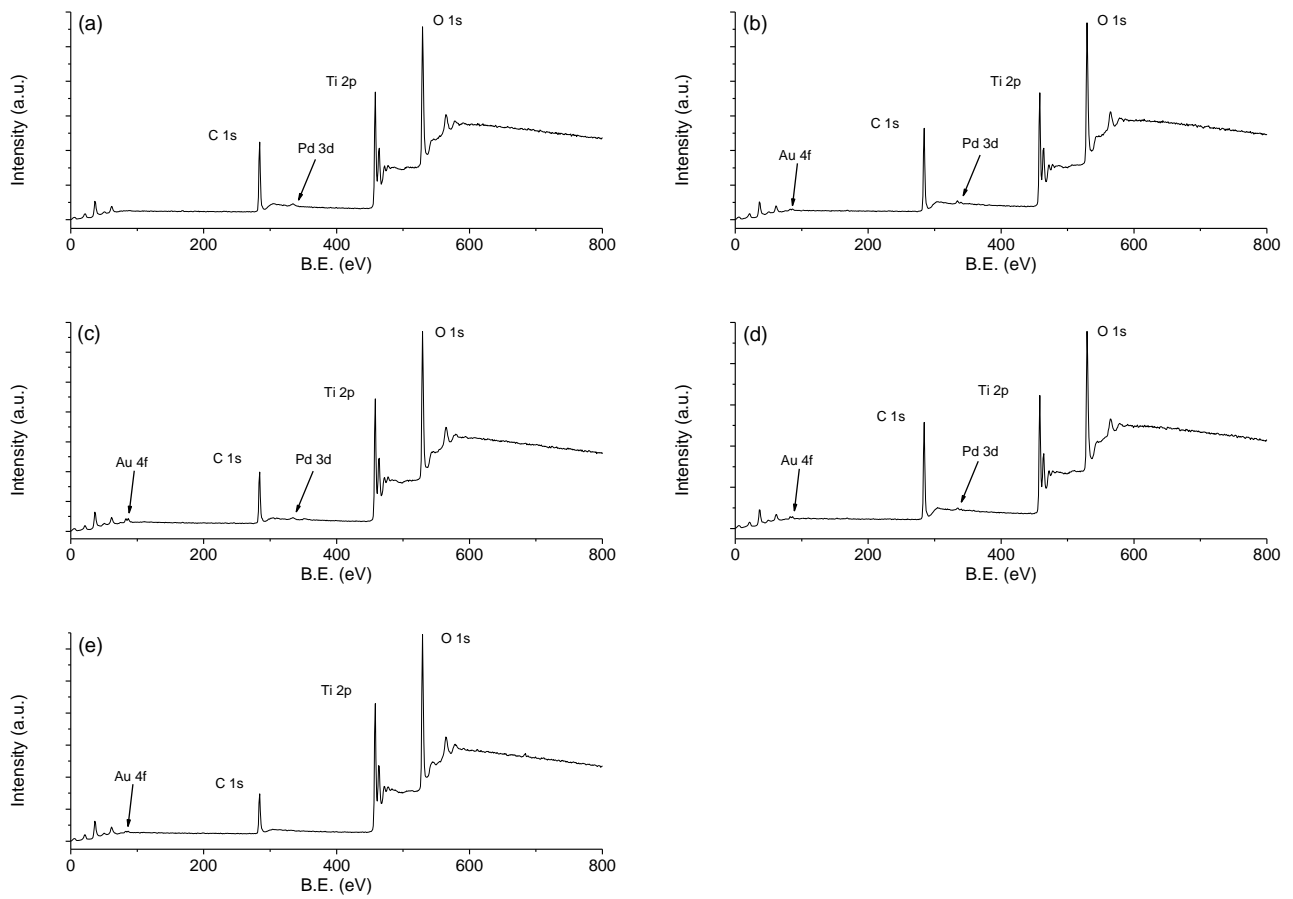


Figure S10: XPS survey scans for the batch-prepared catalysts. (a) Pd/TiO₂, (b) Au₂₅Pd₇₅/TiO₂, (c) Au₅₀Pd₅₀/TiO₂, (d) Au₇₅Pd₂₅/TiO₂ and (e) Au/TiO₂.

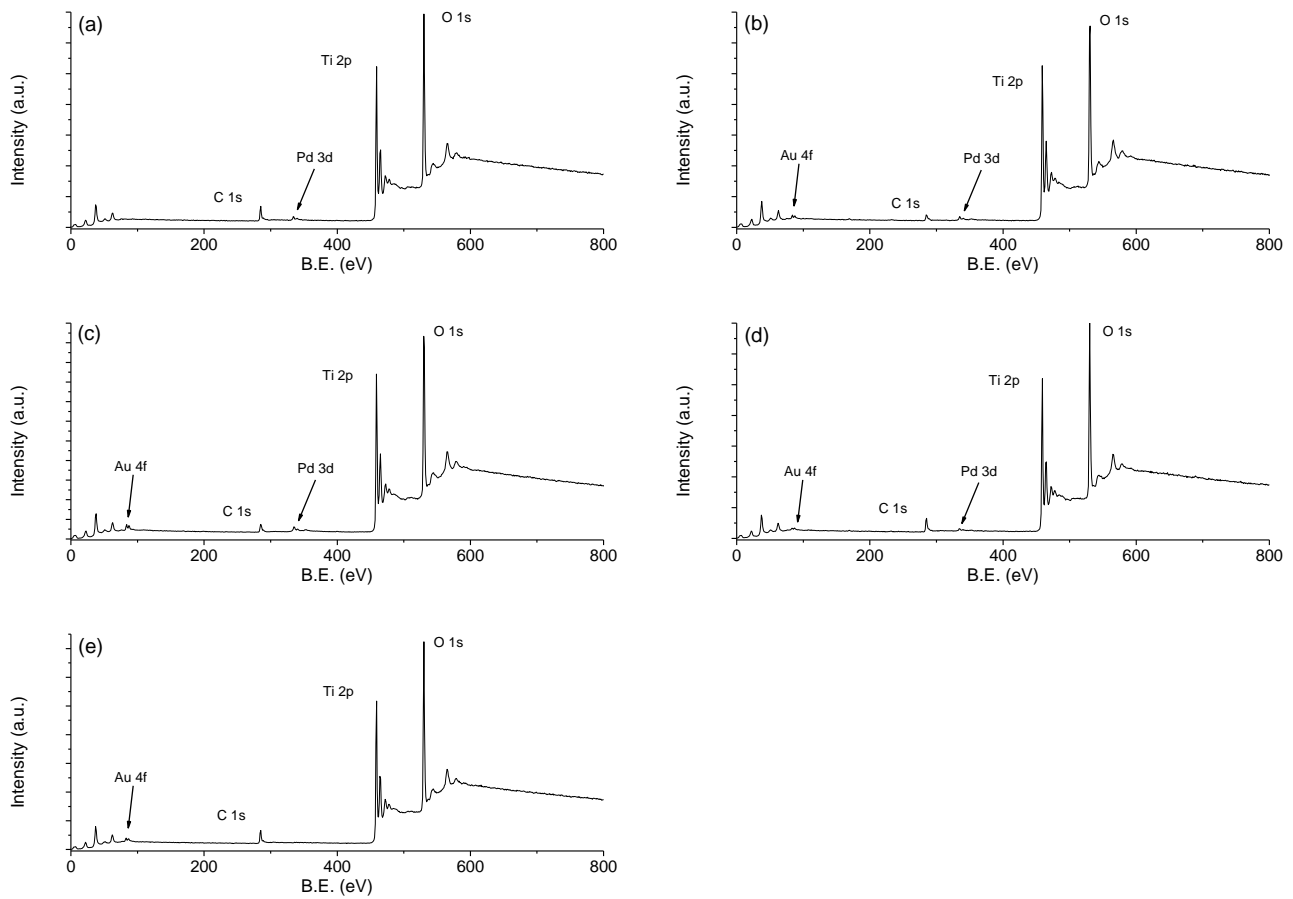


Figure S11: XPS survey scans for the continuous-prepared catalysts. (a) Pd/TiO_2 , (b) $\text{Au}_{25}\text{Pd}_{75}/\text{TiO}_2$, (c) $\text{Au}_{50}\text{Pd}_{50}/\text{TiO}_2$, (d) $\text{Au}_{75}\text{Pd}_{25}/\text{TiO}_2$ and (e) Au/TiO_2 .

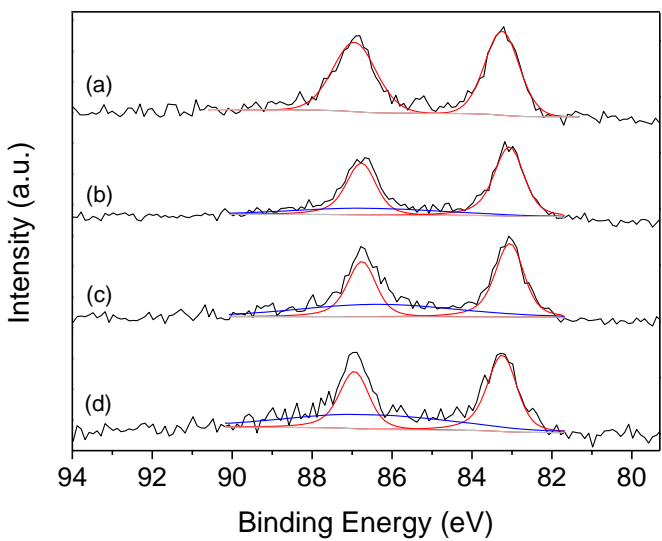


Figure S12: $\text{Au}4f$ XPS analysis of the continuous-prepared $\text{Au}_{75}\text{Pd}_{25}/\text{TiO}_2$ catalysts heat treated at different temperature. (a) untreated, (b) 200 °C, (c) 300 °C and (d) 400 °C. The red fitting represents the Au^0 , while the blue fitting represents the satellite $\text{Pd} 4s$ peak.

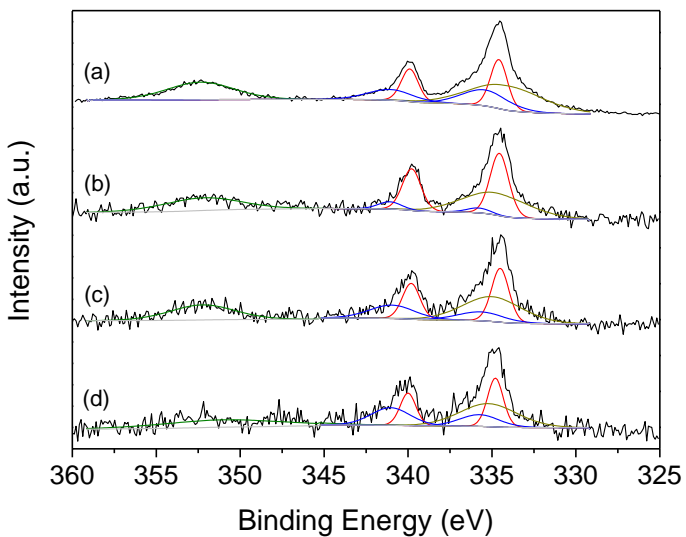


Figure S13: $\text{Pd}3d$ XPS analysis of the continuous-prepared $\text{Au}_{75}\text{Pd}_{25}/\text{TiO}_2$ catalysts heat treated at different temperature. (a) untreated, (b) 200 °C, (c) 300 °C and (d) 400 °C. The red fitting represents the Pd^0 , while the blue fitting represents the Pd^{2+} ; the green fitting represents the satellite $\text{Au} 4d$ peaks.

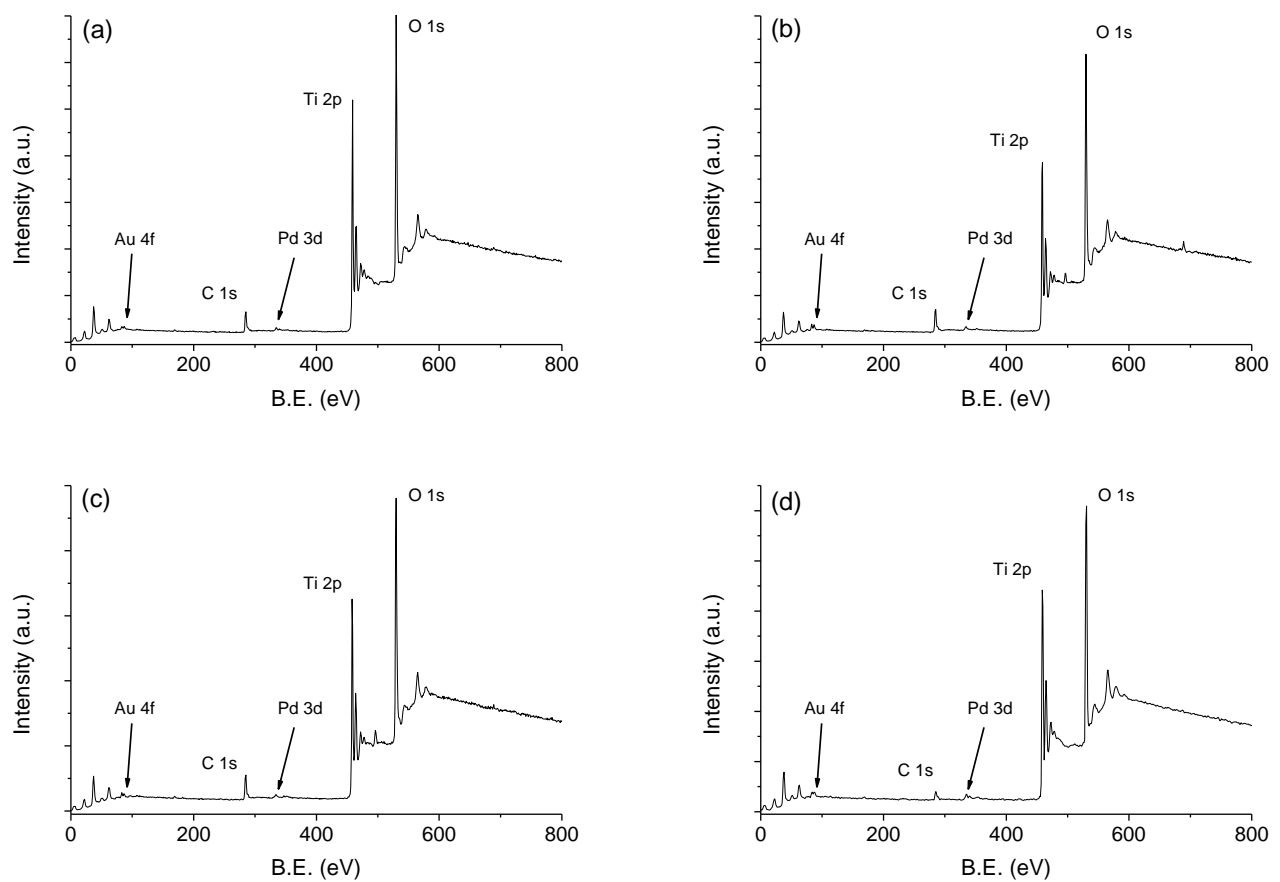


Figure S14: XPS survey scans for the continuous-prepared $\text{Au}_{75}\text{Pd}_{25}/\text{TiO}_2$ catalysts heat treated at different temperature. (a) untreated, (b) $200\text{ }^\circ\text{C}$, (c) $300\text{ }^\circ\text{C}$ and (d) $400\text{ }^\circ\text{C}$.

Table S1: Au:Pd molar ratio and Au 4f_{7/2} and Pd 3d_{5/2} binding energy of the catalysts prepared in continuous (Au₇₅Pd₂₅/TiO₂-C) heat treated at different temperature. The ratios are calculated from XPS quantification.

Catalyst	Au:Pd ratio (mol/mol)	Binding Energy (eV)	
		Au 4f _{7/2}	Pd 3d _{5/2}
Au ₇₅ Pd ₂₅ /TiO ₂ -C	76 : 24	83.2	334.7
Au ₇₅ Pd ₂₅ /TiO ₂ -C-200	72 : 28	83.1	334.7
Au ₇₅ Pd ₂₅ /TiO ₂ -C-300	70 : 30	83.1	334.6
Au ₇₅ Pd ₂₅ /TiO ₂ -C-400	71 : 29	83.2	334.8